RESEARCH ARTICLE | OCTOBER 07 2024

Substrate topography regulating membrane adhesion mediated by receptor–ligand bonds

Yuanyuan Ma ; Long Li ; Ana-Sunčana Smith

Appl. Phys. Lett. 125, 153701 (2024)
https://doi.org/10.1063/5.0224078

Applied Physics Letters ARTICLE pubs.aip.org/aip/apl

Substrate topography regulating membrane adhesion mediated by receptor–ligand bonds

Cite as: Appl. Phys. Lett. **125**, 153701 (2024); doi: 10.1063/5.0224078
Submitted: 19 June 2024 · Accepted: 24 September 2024 ·
Published Online: 7 October 2024

Yuanyuan Ma,[1] Long Li,[1,a)] and Ana-Sunčana Smith[2,3,a)]

AFFILIATIONS

[1]Key Laboratory of Mechanics on Disaster and Environment in Western China, Ministry of Education, College of Civil Engineering and Mechanics, Lanzhou University, Lanzhou, 730000 Gansu, China
[2]PULS Group, Institute for Theoretical Physics and Interdisciplinary Center for Nanostructured Films, Friedrich Alexander University Erlangen-Nürnberg, Erlangen 91058, Germany
[3]Group for Computational Life Sciences, Division of Physical Chemistry, Ruđer Bošković Institute, Zagreb 10000, Croatia

[a)]**Authors to whom correspondence should be addressed:** longl@lzu.edu.cn and smith@physik.uni-erlangen.de

ABSTRACT

Cell adhesion can be significantly influenced by the topography of the substrate surface. However, how the adhesion molecules essentially respond to this topographical stimulus is not fully understood yet. Here, we employ an effective Monte Carlo simulation to systematically investigate a fluctuating membrane interacting with a curved substrate via adhesive proteins. Interestingly, results show that, compared with the flat substrate, curved substrates regulate the membrane adhesion in a bond length dependent manner. The effects of the substrate surface amplitude and wavelength on the number of molecular bonds and adhesion pattern are also extracted from the scaling relationship between the characteristic lateral length of the membrane and the local substrate curvature radius. Furthermore, the local substrate curvature is found to select the bond distribution in terms of the bond length and stiffness. The results suggest that the bond stiffness enhances the clustering of molecular bonds, mainly due to synergistic interactions among these molecular bonds.

Cell adhesion mediated by receptor–ligand binding serves as a fundamental process that intricately regulates essential cellular activities, such as proliferation, differentiation, migration, and tissue formation.[1,2] In biological systems, cell adhesion interfaces often have a complex surface topography, instead of a pretty flat surface. Characteristic circumstances are the basement membrane with rich nano-topographies in tissues directly interacting with adjacent cells[3] and the formation of extracellular matrix fibrils tens of micrometers in length and a few hundred nanometers in diameter presenting a complex topographical structure.[4] Concerning these topographical environments surrounding adherent cells, extensive experimental observations *in vitro* suggest that the cell adhesion behaviors (e.g., spreading, orientation, and migration) are strikingly sensitive to the substrate topography.[5–13] Specifically, culturing cells on a flat substrate and a substrate with micropatterned morphology surface, respectively, demonstrates that the substrate microtopography would promote the formation and maturation of focal adhesion.[14] Moreover, the microwavy patterned substrate surfaces could obviously increase the adhesion strength and the cell alignment.[15] In addition to the micropattern of the substrate surface, the roughness of the substrate surface emerges as another crucial factor modulating the cell–substrate interaction.[16–19] In particular, regarding osteoblasts and neural cells, their viability and size would first increase and then decrease as surface roughness increases. Despite such remarkable influence of substrate topography on cell adhesion, there are only scarce attempts to understand how the adhesion molecules respond to this topographical cue. Recent works[20,21] taking into account membrane adhesion only mediated by rigid adhesive proteins have explored the response of a membrane to a curved substrate and lipid effects. Nevertheless, the nonspecific interaction also significantly regulates the membrane adhesion[22] and the adhesive molecules exhibit rich biomechanical properties as experimentally observed.[23] Additionally, even for cells adhering to a flat substrate, previous works suggested that the adhesion system could be also affected by the cooperativity between molecular bonds.[24–26] The difficulty here in describing the interaction between the cell and the curved substrate arises from coupling between the substrate topography and the mechanical properties of molecular bonds and the fluctuating membrane.

Here, referring to cell mimetic systems consisting of giant monolayer vesicles adhering to substrates, we extend a recently developed

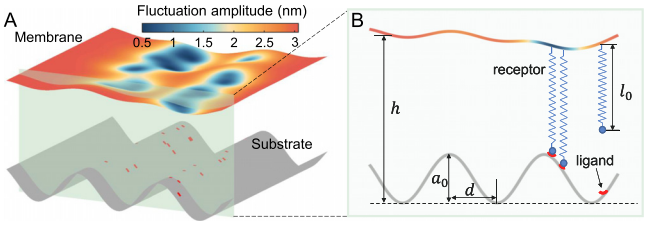

FIG. 1. Schematic diagram of a fluctuating membrane interacting with a curved substrate via a set of adhesive molecules. (a) The formation of adhesive bonds as labeled by the red dots deforms the membrane. The color bar stands for the fluctuation amplitude of membrane. (b) The cross-sectional diagram [as marked by light green in (a)] of the membrane–substrate system is provided. The membrane height and the rest length of adhesive molecule are denoted as h and l_0, respectively. The surface topography of the curved substrate is determined by the height $h_s = \frac{a_0}{2}\left(\sin\frac{\pi x}{d} + 1\right)$ with amplitude a_0 and half-wavelength d.

Monte Carlo scheme[27] for simulating a fluctuating membrane interacting with a flat substrate to investigate the effect of substrate topography on membrane adhesion through a series of receptor–ligand bonds as schematically depicted in Fig. 1, where the molecular bonds are treated as thermal harmonic springs. The unbound receptors and ligands are coated on the surfaces of membrane and substrate, respectively. In addition to the specific interplay between adhesive molecules, the membrane adhesion process is also attributed to nonspecific factors containing van der Waals and Coulomb interactions as well as hydration between the membrane and curved substrate surfaces. Subsequently, the free energy of a fluctuating membrane adhering to a curved substrate can be written by the Helfrich Hamiltonian as a function of membrane height $h(\mathbf{r})$,[27–29]

$$\mathscr{H}[h(\mathbf{r})] = \int_S d^2\mathbf{r}\left\{\frac{\kappa}{2}\left(\nabla^2 h(\mathbf{r})\right)^2 + \frac{\gamma}{2}[h(\mathbf{r}) - h_s(\mathbf{r}) - h_0]^2\right\} + \sum_{i=1}^{n}\delta(\mathbf{r} - \mathbf{r}_i)\left[\frac{\lambda}{2}[h(\mathbf{r}) - h_s(\mathbf{r}) - l_0]^2 - \varepsilon_b\right], \quad (1)$$

where the first term describes the bending energy of the elastic membrane upon treating the membrane mean curvature in the Monge representation with bending stiffness κ, the second term showing a harmonic potential of strength γ with a minimum at h_0 reflects the nonspecific interaction maintaining a separation between the membrane and substrate surfaces, and the last term accounts for the binding energy, ε_b, and the elastic energy of bond with stiffness, λ, as a result of the formation of n receptor–ligand bonds.

Considering the membrane height following the Boltzmann distribution, we can semi-analytically obtain the membrane height distribution, $p[h(\mathbf{r})]$, with respect to the above expressed free energy in Eq. (1) through a rigorous field theory processing as previously presented[27,29] (see the supplementary material for details). Indeed, such a membrane height distribution appearing in the form of a Gaussian distribution with the mean membrane height and the fluctuation amplitude explicitly takes into account not only the bond position and biomechanics but also the substrate topography (see the supplementary material for membrane height distribution). Once the membrane height distribution is obtained, regarding the association/dissociation of molecular bond, the correspondingly effective binding/unbinding rates coupled to the membrane fluctuation can be defined as $K_{on} \equiv \int dh p(h) k_{on}(h)$ and $K_{off} \equiv \int dh p(h) k_{off}(h)$ with instantaneous reaction rates k_{on} and k_{off}[27] (see the supplementary material). To simulate the dynamic evolution of the fluctuating membrane interacting with the curved substrate, extending the recently developed Monte Carlo scheme of membrane adhesion,[27,29,30] we discretize both the membrane and the substrate surfaces into a series of square lattices with a constant a, in which each lattice could host a receptor or a ligand molecule. Moreover, a rectangular contact region is considered (see Fig. S1 in the supplementary material). Initially, the free receptors and their ligands are randomly positioned on the two surfaces, respectively. As random walkers, both the freely mobile receptors and ligands can arbitrarily move on the surfaces of membrane and substrate under periodic boundary conditions, respectively. Nevertheless, once the receptor–ligand pair forms a bond within the contact zone, such bound receptor and ligand are immobile. The condition of constant density of receptor and ligand in the free area is considered here and provides the reservoir reconstructing the appropriate statistical ensemble. In the current context, using periodic boundary conditions could provide homogeneous reservoirs at the finite free regions of the simulation system. However, when the membrane interacting with the substrate is subjected to the constant amounts of receptor and ligand molecules (corresponding to a finite reservoir of adhesive binders), reflecting boundary conditions, rather than the periodic boundary conditions, are required.

During each simulation step, the random motion of free receptors/ligands and binding/unbinding processes of adhesive pairs are performed sequentially. Please see the supplementary material for a detailed description of Monte Carlo simulations. Taking the representative values of the related parameters in the Monte Carlo simulations as summarized in the supplementary material, the dynamic response of adhesive molecules to the curved substrate surface can be achieved by implementing the above simulation process.

Figure 2(a) shows the representative results of the effect of substrate topography on the number of closed bonds evolving over time for short ($l_0 = 30$ nm) and long ($l_0 = 50$ nm) bonds, respectively. It can be seen that the membrane adhesion system rapidly reaches thermodynamic equilibrium from an initial non-bond forming state and the curved substrate notably regulates the amount of adherent bonds in a bond length dependent manner. Interestingly, a membrane interacting with a flat substrate through short adhesive binders with length, 30 nm, is associated with transient formations of sporadic molecular bonds that exhibit unstable membrane adhesion. However, in the case of the curved substrate, these short binders would form molecular bonds in relatively large quantities, clustering at the crest of the curved substrate [see inset in Fig. 2(a)]. This finding indicates that the substrate topography obviously promotes membrane adhesion regulated by short binders. This is because the curved substrate presents small interfacial distances at its peaks [Fig. 2(b)] that increase the effective binding affinity of receptor–ligand binding. In contrast to the circumstance of the short adhesive binder, the formation of the long adhesive binders modulating the membrane adhesion is evidently suppressed at the troughs of the curved substrate [see inset in Fig. 2(a)], compared to that on a flat substrate. This is because the effective adhesive region for the formation of long receptor-ligand bond is reduced at the troughs of the curved substrate corresponding to large interfacial distances [Fig. 2(b)]. These substrate topography effects relying on the bond length are mainly attributed to coupling between the adhesive binder

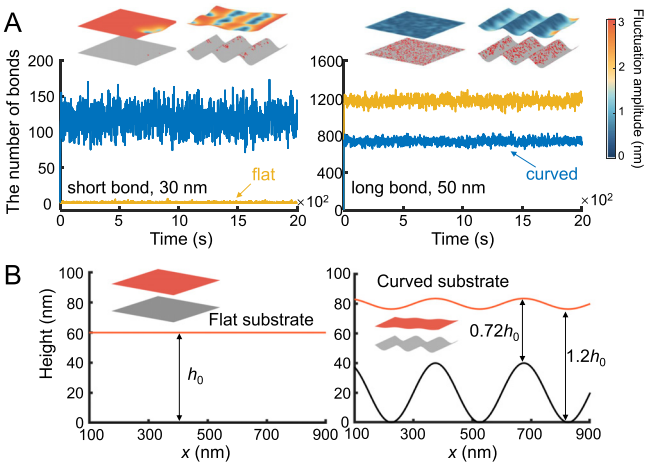

FIG. 2. (a) Evolution of the number of closed bonds for membrane adhesion mediated by a short bond of $l_0 = 30$ nm (left panel) and long bond of $l_0 = 50$ nm (right panel), respectively. The insets present snapshots of the thermodynamic equilibrium states of the membrane interacting with flat and curved ($a_0 = 40$ nm and $d = 150$ nm) substrates for different binder lengths (30 and 50 nm), respectively. (b) Membrane profile for the initial non-adherent state of the membrane–substrate system where the membrane deformation completely results from nonspecific interaction.

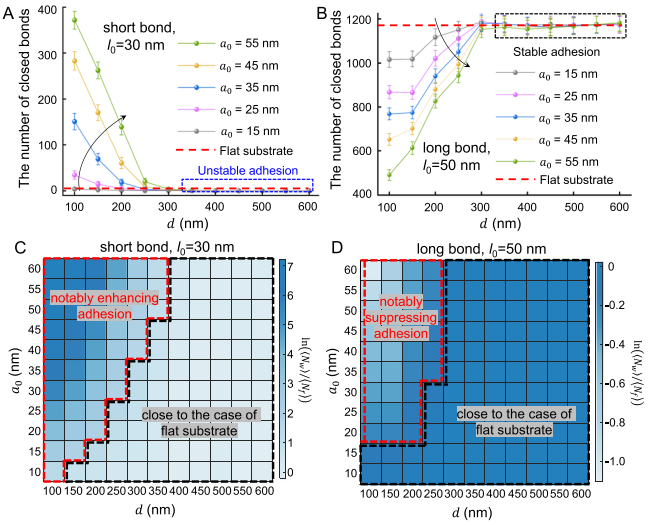

FIG. 3. The number of bound receptor–ligand bonds at thermodynamic equilibrium of the membrane adhering to a series of curved substrates with different morphologies determined by the amplitude a_0 and the half-wavelength d, in the case of (a) short and (b) long binders. The black arrows represent increasing the amplitude a_0 of the curved substrate surface. Phase diagram of the average number of bound bonds as a function of the amplitude a_0 and half-wavelength d of the curved substrate surface for (c) short and (d) long binders.

reaction, membrane/substrate separation as well as membrane deformation.

To further explore the effects of substrate topography on the thermodynamic equilibrium of membrane adhesion in the extended range, we systematically calculated the number of bound bonds as a function of the amplitude a_0 and the half-wavelength d for short and long binders, as plotted in Figs. 3(a) and 3(b). In the range of small half-wavelengths of the curved substrate, it can be seen that the number of binders scales linearly with wavelength due to a combination of the number of peaks and the geometric characteristics of these peaks, as the latter would affect the localized effective adhesion area of each peak and the separation between the membrane and the curved substrate surfaces. In addition, during short binder mediated membrane adhesion, for a given small wavelength of the curved substrate, as the substrate amplitude increases, the number of closed bonds would become large due to a high amplitude associated with a small interfacial distance at the substrate peaks subjected to nonspecific interaction (see Fig. S2 in the supplementary material), resulting in short binders readily forming bonds. Meanwhile, this curved substrate surface with high amplitude and small wavelength also induces a large interfacial distance at substrate troughs in which even for relatively long binders of $l_0 = 50$ nm, in the current context, the binding of adhesive binders is not strong enough to drive membrane pinning due to large elastic deformations of the membrane. As such, a high amplitude would significantly inhibit long bond formation at substrate troughs for a small wavelength. Nevertheless, with increasing wavelength of the curved substrate surface, in the case of both the short and long binders, the number of bound bonds exhibits non-dependence on the substrate amplitude and its value is close to that of the membrane adhering to a flat substrate. This membrane–substrate interaction irrespective of the substrate amplitude is caused by the scaling relationship between the characteristic lateral correlation length of the membrane and the larger curvature radius of the substrate surface in which the membrane profile matches the substrate morphology well with separation h_0 during initial non-bond forming state (see Fig. S1 in the supplementary material). Moreover, there is a cutoff value for the wavelength of the curved substrate above which the number of closed bonds does not change and is approximately equivalent to that calculated in the case of the membrane interacting with a flat substrate [see Figs. 3(a) and 3(b)]. This critical wavelength of the curved substrate is also a result of the scaling relationship between the characteristic lateral length of the membrane and the local substrate curvature radius. In principle, the characteristic lateral length of the membrane is a length scale of the membrane deformation. For the tensionless membrane as considered in the current context, the characteristic lateral length of the membrane coupling the strength of the nonspecific potential can be explicitly defined as $\sqrt[4]{\kappa/\gamma}$.[27] For the case when the curved substrate's wavelength is larger than the critical value, the local substrate curvature radius is also much larger than the membrane's characteristic lateral length. In such a situation, it seems that the membrane becomes soft so that the membrane profile is tightly adapted to the substrate topology under the nonspecific interaction. Specifically, the interface separation of the membrane–substrate system only mediated by nonspecific interaction is calculated to be almost uniformly h_0 as shown in Fig. S2 (a) in the supplementary material. As such, local binding of the adhesion bonds is analogous to that as simulated in the flat substrate case. Nevertheless, when the wavelength of the curved substrate is much smaller than the critical value, the characteristic lateral length of the membrane is much larger than the local substrate curvature radius. It appears that the membrane becomes stiff, indicating the nonspecific potential cannot substantially deform the membrane to match the substrate morphology well. Furthermore, a normalized number $\ln(\langle N_w\rangle/\langle N_f\rangle)$ with the average number of bound bonds in the case

of curved and flat substrates being $\langle N_w \rangle$ and $\langle N_f \rangle$, respectively, is determined to evaluate the effect of the curved substrate topography on the formation of molecular bonds for short and long binders, as shown in Figs. 3(c) and 3(d), respectively.

Additionally, we consider a curved substrate with exponentially decaying amplitude (see Fig. 4) corresponding to a more complex scenario of substrate topography. In such a case of curved substrate, the bond distribution relying on the bond length is analyzed as plotted in Fig. 4. During the initial non-bond forming state, the membrane deformed by nonspecific interaction as an approximate plane associated with high interfacial distances within the region of low amplitude of the curved substrate. For the membrane pinned to the curved substrate by a series of adhesive bonds, it is found that as the bond length increases, the distribution of bond formation gradually changes from peaks to troughs and mainly transforms from high to low amplitudes of the curved substrate due to a minimal free energy of the membrane adhesion system.

Additionally, we also examine the impact of bond stiffness on the membrane interacting with a curved substrate, as the interface behavior among cell adhesion is sensitive to the elasticity of molecular bonds in biological systems.[31,32] Figure 5(a) displays the effect of bond stiffness on the evolution of the number of bonds with time during the interaction between the membrane and the curved substrate via a set of adhesive binders with distinct lengths. It can be seen that the number of bonds monotonously increases and eventually converges to

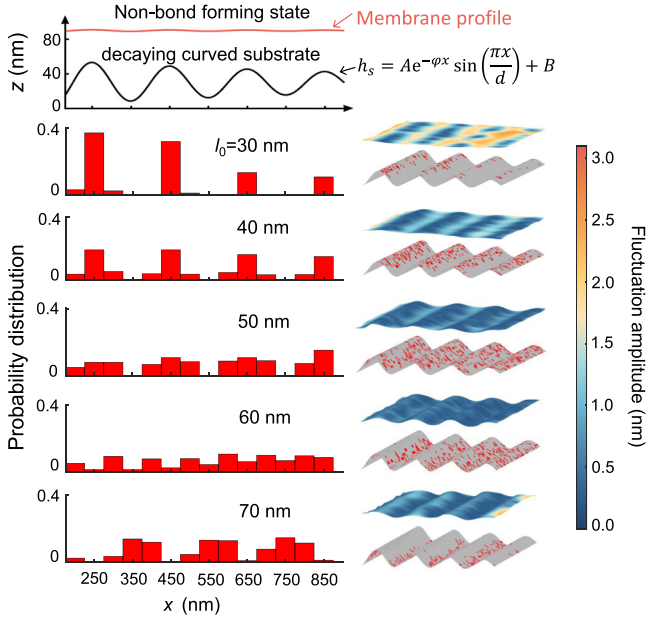

FIG. 4. Fluctuating membrane adhering to a curved substrate with exponentially decaying amplitude ($A = 30$ nm, $\varphi = 0.01\,\text{nm}^{-1}$, $d = 100$ nm, and $B = 30$ nm) for different adhesive binder lengths at thermodynamic equilibrium states. At initial non-bond forming state, the membrane profile induced by the nonspecific interaction between membrane and substrate is theoretically calculated as displayed in the top. A set of histograms indicate the probability distribution of the bound bonds on the substrate surface for membrane adhesion modulated by different receptor–ligand bonds with distinct lengths. Their associated simulation snapshots of membrane–substrate system are shown on the right.

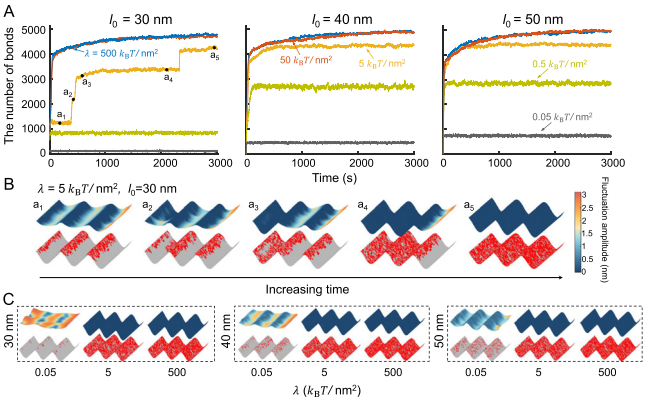

FIG. 5. Effect of bond stiffness on membrane interacting with a curved substrate at $a_0 = 40$ nm and $d = 150$ nm. (a) Evolution of the number of closed bonds with time for different bond stiffnesses and bond lengths. $a_1 - a_5$ stand for the representative configuration states of the membrane/substrate system chosen from simulated trajectory of bond length 30 nm and bond stiffness $5\,k_BT/\text{nm}^2$. (b) The related simulation snapshots of the membrane/substrate system evolving with the points in time series $a_1 - a_5$. (c) Snapshots of the membrane/substrate system at thermodynamic equilibrium as a function of bond stiffness for different bond lengths.

constant values with increasing bond stiffness at a fixed time point, which apparently reflects the bond stiffness improving the formation of adhesive binders irrespective of their length. In addition to the evolution of the bond number, snapshots of the membrane adhering to the curved substrate evolving with a series of time points are exhibited in Fig. 5(b), in which $a_1 - a_5$ are representative system configuration states chosen from the simulation trajectory of $\lambda = 5\,k_BT/\text{nm}^2$ and $l_0 = 30$ nm as labeled in Fig. 5(a). Moreover, the related simulation snapshots of membrane adhesion reaching thermodynamic equilibrium as a function of bond stiffness for different bond lengths are shown in Fig. 5. It can be seen that the elastic membrane can be adequately pinned by stiff adhesive bonds. Indeed, the bond stiffness promoting the formation of adhesive binders is a result of cooperative interaction between neighboring molecular bonds. Although a stiff bond corresponds to small oscillation under thermal stimulation, during the adhesion process of the membrane–substrate system, the stiff bond formation can pin the elastic membrane with a relatively large deformation around the binding site. As such, this profile of the pinned membrane by the stiff bond gives rise to a relatively small distance between the membrane and substrate surfaces around the binding site. This reduction in the membrane–substrate distance around the adhesion sites allows more adjacent bonds to bind more readily, thereby improving the formation of bonds and increasing the total number of bonds formed. In this cooperative manner of adhesive bonds, typically the adhesion domains of stiff bonds develop from initial nucleation at the substrate peaks to growth toward the substrate troughs [please see Fig. 5(b)]. Nevertheless, this cooperative effect becomes insignificant for soft bonds during membrane adhesion, since the formation of soft bonds cannot obviously deform the membrane. Recent theoretical effort concerning the adhesive contact between cells and a wavy extracellular matrix mediated by receptor–ligand bonds suggests a similar effect of bond stiffness on cell adhesion, in which the bond stiffness would enhance the adhesion strength at high roughness of the substrate surface,[32] probably due to the elastic adhesive interface

consisting of stiff receptor–ligand bonds corresponding to relatively uniform interfacial forces. Alternatively, the present work describing a fluctuating membrane interacting with a curved substrate via molecular bonds provides another concept of bond stiffness influencing cell adhesion.

In summary, we extend a recently developed Monte Carlo scheme of a fluctuating elastic membrane interacting with a flat substrate to explore the topography of a curved substrate affecting membrane adhesion through a series of adhesive protein binders. Through examining the evolution of the number of bonds formed by these binders and the adhesion pattern as a function of bond length for flat and curved substrates, respectively, it is found that the curved substrates regulate membrane adhesion in a bond length dependent manner. In particular, a curved substrate with a highly curved surface (high amplitude and low wavelength) promotes the formation of short binders at its peaks and suppresses the formation of long binders at its troughs due to the nonspecific interaction resulting in low and high membrane–substrate separation at the peaks and troughs of the curved substrate, respectively. Furthermore, extending the range of amplitude and wavelength of the curved substrate suggests that the results of membrane adhesion tend to be similar to those occurring in the case of flat substrates as the surface wavelength of the substrate increases, regardless of amplitude. This is because the membrane's characteristic lateral length is much smaller than the radius of substrate surface curvature at large wavelengths. It is also found that increased bond stiffness would promote cluster development of receptor–ligand bonds due to synergistic interactions among molecular bonds.

Membrane adhesion plays an essential role in many biological processes. Indeed, membrane–substrate interaction is a complex biophysical process and involves a variety of essential factors, such as receptor–ligand binding, nonspecific potential,[22] membrane fluctuation,[33] substrate topography[16] as well as biomechanics of receptor–ligand bonds.[23,34–36] However, how these factors are properly accounted for, combined, and eventually formed into an effective computational model will be crucial. Exploring the potential biophysical mechanism behind this complex interrelationship provides a fundamental understanding of membrane adhesion in biological systems. A recent study computationally elucidated the interplay between fluctuating membranes and corrugated or egg-carton shaped substrate via the binding of rigid adhesive binders.[20] It is found that increasing the profile height of the substrate would significantly reduce the effective binding affinity of adhesive binders, indicating that the substrate topography appropriately suppresses membrane adhesion. This is because the binding energy of adhesive binders cannot substantially drive the large membrane deformation to match the substrate topography with local high curvature. For the effect of membrane lipids, it is further identified that the substrate topography has the potential to enhance the condensation of receptors associated with lipid nanodomains.[21] Although these findings contribute to improving the understanding of membrane adhesion, it is necessary to explore how the fluctuating membrane responds to the substrate topography in a more realistic scenario where both the nonspecific interaction and the biomechanics of the molecular bonds (e.g., the rest length and the stiffness) are inherently linked to the membrane adhesion system. A recently developed Kinetic Monte Carlo scheme,[27] with higher computational efficiency than the previous Monte Carlo method,[20,21] is used to computationally investigate how the membrane adhesion responds to the substrate morphology at the molecular bond level. In contrast to the results as predicted in the previous work,[20] we find the curved substrates regulating membrane adhesion in a bond length dependent manner rather than always inhibiting the formation of molecular bonds. Moreover, it is examined that the nonspecific interaction and biomechanics of adhesive binders are crucial for the substrate topography regulating membrane adhesion mediated by receptor–ligand bonds. These findings provide biophysical insight into the mechanism of substrate topography as a physical cue guiding membrane adhesion by coupling the nonspecific interaction and biomechanics of adhesive binders.

See the supplementary material for details on the calculation of the probability distribution of membrane height, the kinetic Monte Carlo method for membrane–substrate interaction, and additional results of the membrane–substrate system profile for different substrate topographies at initial non-bonding stages.

This study is supported by grants from the National Natural Science Foundation of China (Nos. 12072137 and 12472162), the Fundamental Research Funds for the Central Universities (Grant No. lzujbky-2023-03), the Open Fund of Key Laboratory for Intelligent Nano Materials and Devices of the Ministry of Education NJ2020003 (No. INMD-2021M03), and the German Research Foundation (No. DFG SM 289/10-1). The authors would like to thank the anonymous referees for their comprehensive and constructive comments.

AUTHOR DECLARATIONS

Conflict of Interest

The authors have no conflicts to disclose.

Author Contributions

Yuanyuan Ma: Data curation (lead); Formal analysis (lead); Investigation (equal); Methodology (supporting); Validation (equal); Visualization (lead); Writing – original draft (lead); Writing – review & editing (supporting). **Long Li:** Conceptualization (equal); Formal analysis (supporting); Funding acquisition (lead); Investigation (equal); Methodology (equal); Project administration (lead); Supervision (lead); Validation (equal); Writing – review & editing (lead). **Ana-Sunčana Smith:** Conceptualization (equal); Investigation (equal); Methodology (lead); Resources (lead); Software (lead); Writing – review & editing (supporting).

DATA AVAILABILITY

The data that support the findings of this study are available from the corresponding authors upon reasonable request.

REFERENCES

[1]K. Vleminckx and R. Kemler, "Cadherins and tissue formation: Integrating adhesion and signaling," Bioessays **21**, 211–220 (1999).
[2]T. Okegawa, R.-C. Pong, Y. Li, and J.-T. Hsieh, "The role of cell adhesion molecule in cancer progression and its application in cancer therapy," Acta Biochim. Pol. **51**, 445–457 (2004).
[3]G. Abrams, S. Goodman, P. Nealey, M. Franco, and C. Murphy, "Nanoscale topography of the basement membrane underlying the corneal epithelium of the rhesus macaque," Cell Tissue Res. **299**, 39–46 (2000).
[4]L. Bozec, G. van der Heijden, and M. Horton, "Collagen fibrils: Nanoscale ropes," Biophys. J. **92**, 70–75 (2007).

[5]C. J. Bettinger, R. Langer, and J. T. Borenstein, "Engineering substrate topography at the micro-and nanoscale to control cell function," Angew. Chem. Int. Ed. **48**, 5406–5415 (2009).
[6]R. G. Flemming, C. J. Murphy, G. A. Abrams, S. L. Goodman, and P. F. Nealey, "Effects of synthetic micro-and nano-structured surfaces on cell behavior," Biomaterials **20**, 573–588 (1999).
[7]D. D. Deligianni, N. D. Katsala, P. G. Koutsoukos, and Y. F. Missirlis, "Effect of surface roughness of hydroxyapatite on human bone marrow cell adhesion, proliferation, differentiation and detachment strength," Biomaterials **22**, 87–96 (2000).
[8]G. Zhao, O. Zinger, Z. Schwartz, M. Wieland, D. Landolt, and B. D. Boyan, "Osteoblast-like cells are sensitive to submicron-scale surface structure," Clin. Oral Implants Res. **17**, 258–264 (2006).
[9]M. J. P. Biggs, R. G. Richards, and M. J. Dalby, "Nanotopographical modification: A regulator of cellular function through focal adhesions," Nanomed.: Nanotechnol., Biol. Med. **6**, 619–633 (2010).
[10]A. M. Ross, Z. Jiang, M. Bastmeyer, and J. Lahann, "Physical aspects of cell culture substrates: Topography, roughness, and elasticity," Small **8**, 336–355 (2012).
[11]M. Ventre, C. F. Natale, C. Rianna, and P. A. Netti, "Topographic cell instructive patterns to control cell adhesion, polarization and migration," J. R. Soc. Interface **11**, 20140687 (2014).
[12]A. T. Nguyen, S. R. Sathe, and E. K. Yim, "From nano to micro: Topographical scale and its impact on cell adhesion, morphology and contact guidance," J. Phys.: Condens. Matter. **28**, 183001 (2016).
[13]S. Cai, C. Wu, W. Yang, W. Liang, H. Yu, and L. Liu, "Recent advance in surface modification for regulating cell adhesion and behaviors," Nanotechnol. Rev. **9**, 971–989 (2020).
[14]C. H. Seo, K. Furukawa, K. Montagne, H. Jeong, and T. Ushida, "The effect of substrate microtopography on focal adhesion maturation and actin organization via the RHoA/ROCK pathway," Biomaterials **32**, 9568–9575 (2011).
[15]J. Hu, C. Hardy, C.-M. Chen, S. Yang, A. S. Voloshin, and Y. Liu, "Enhanced cell adhesion and alignment on micro-wavy patterned surfaces," PLoS One **9**, e104502 (2014).
[16]Y. Fan, F. Cui, S. Hou, Q. Xu, L. Chen, and I.-S. Lee, "Culture of neural cells on silicon wafers with nano-scale surface topograph," J. Neurosci. Methods **120**, 17–23 (2002).
[17]S. P. Khan, G. G. Auner, and G. M. Newaz, "Influence of nanoscale surface roughness on neural cell attachment on silicon," Nanomed.: Nanotechnol., Biol. Med. **1**, 125–129 (2005).
[18]D. Khang, J. Lu, C. Yao, K. M. Haberstroh, and T. J. Webster, "The role of nanometer and sub-micron surface features on vascular and bone cell adhesion on titanium," Biomaterials **29**, 970–983 (2008).
[19]H. Kim, S. Kim, M. Kim, E. Lee, H. Oh, W. Oh, S. Park, W. Kim, G. Lee, N. Choi *et al.*, "Varying Ti-6Al-4V surface roughness induces different early morphologic and molecular responses in MG63 osteoblast-like cells," J. Biomed. Mater. Res. **74A**, 366–373 (2005).
[20]L. Li, J. Gao, Y. Shao, F. Song, and J. Hu, "Tuning cell adhesion on supported lipid bilayers via nanoscale geometry," Soft Matter **17**, 10376–10382 (2021).
[21]L. Li, R. Hou, X. Shi, J. Ji, B. Różycki, J. Hu, and F. Song, "Control of cell membrane receptor condensation by adhesion to supported bilayers with nanoscale topography," Commun. Phys. **7**, 174 (2024).
[22]D. Schmidt, C. Monzel, T. Bihr, R. Merkel, U. Seifert, K. Sengupta, and A.-S. Smith, "Signature of a nonharmonic potential as revealed from a consistent shape and fluctuation analysis of an adherent membrane," Phys. Rev. X **4**, 021023 (2014).
[23]A. Janshoff, M. Neitzert, Y. Oberdörfer, and H. Fuchs, "Force spectroscopy of molecular systems—Single molecule spectroscopy of polymers and biomolecules," Angew. Chem. Int. Ed. **39**, 3212–3237 (2000).
[24]T. Erdmann and U. S. Schwarz, "Stability of adhesion clusters under constant force," Phys. Rev. Lett. **92**, 108102 (2004).
[25]T. Speck, E. Reister, and U. Seifert, "Specific adhesion of membranes: Mapping to an effective bond lattice gas," Phys. Rev. E **82**, 021923 (2010).
[26]K. Blom and A. Godec, "Criticality in cell adhesion," Phys. Rev. X **11**, 031067 (2021).
[27]T. Bihr, U. Seifert, and A.-S. Smith, "Multiscale approaches to protein-mediated interactions between membranes—relating microscopic and macroscopic dynamics in radially growing adhesions," New J. Phys. **17**, 083016 (2015).
[28]D. Schmidt, T. Bihr, U. Seifert, and A.-S. Smith, "Coexistence of dilute and densely packed domains of ligand-receptor bonds in membrane adhesion," Europhys. Lett. **99**, 38003 (2012).
[29]T. Bihr, U. Seifert, and A.-S. Smith, "Nucleation of ligand-receptor domains in membrane adhesion," Phys. Rev. Lett. **109**, 258101 (2012).
[30]L. Li, B. H. Stumpf, and A.-S. Smith, "Molecular biomechanics controls protein mixing and segregation in adherent membranes," Int. J. Mol. Sci. **22**, 3699 (2021).
[31]M. J. Whitfield, J. P. Luo, and W. E. Thomas, "Yielding elastic tethers stabilize robust cell adhesion," PLoS Comput. Biol. **10**, e1003971 (2014).
[32]B. Chong, Z. Gong, and Y. Lin, "Modeling the adhesive contact between cells and a wavy extracellular matrix mediated by receptor–ligand interactions," J. Appl. Mech. **84**, 011010 (2017).
[33]S. F. Fenz, T. Bihr, D. Schmidt, R. Merkel, U. Seifert, K. Sengupta, and A.-S. Smith, "Membrane fluctuations mediate lateral interaction between cadherin bonds," Nat. Phys. **13**, 906–913 (2017).
[34]L. Li, M. A. Kamal, B. H. Stumpf, F. Thibaudau, K. Sengupta, and A.-S. Smith, "Biomechanics as driver of aggregation of tethers in adherent membranes," Soft Matter **17**, 10101–10107 (2021).
[35]M. A. Kamal, J. A. Janeš, L. Li, F. Thibaudau, A.-S. Smith, and K. Sengupta, "Physics of organelle membrane bridging via cytosolic tethers is distinct from cell adhesion," Front. Phys. **9**, 750539 (2022).
[36]E. Toledo, G. Le Saux, A. Edri, L. Li, M. Rosenberg, Y. Keidar, V. Bhingardive, O. Radinsky, U. Hadad, C. Di Primo *et al.*, "Molecular-scale spatio-chemical control of the activating-inhibitory signal integration in NK cells," Sci. Adv. **7**, eabc1640 (2021).